Unsupervised Adaptive Background Subtraction in Distributed Radar Target Tracking Systems

Jaya Shradha Fowdur*, Feyza Eksen†, Lucas Paes Moreira*, Paweł Banyś*
*Institute of Communications and Navigation, German Aerospace Center (DLR), Neustrelitz, Germany
†Institute for Visual and Analytic Computing, University of Rostock, Germany
E-mail: {jaya.fowdur, lucas.paesmoreira, pawel.banys}@dlr.de; feyza.eksen@uni-rostock.de

2025 IEEE Radar Conference (RadarConf25) | 979-8-3315-4433-1/25/$31.00 ©2025 IEEE | DOI: 10.1109/RADARCONF2559087.2025.11205131

***Abstract*—Detecting and tracking vessels based on radar sensors in harbours and urban waterways pose multiple challenges due to noise, occlusion, persistent clutter reflections and interference due to infrastructure that affect the target tracking process. To address these challenges, we present a distributed tracking system that fuses data from static and dynamic radars with an unsupervised adaptive background subtraction approach, namely Adaptive Background Subtraction (ABS), for multiple extended target tracking (METT). The findings and benefits of our proposed framework are demonstrated through custom maritime simulated traffic scenarios with appropriate evaluation schemes. In addition, we illustrate the initial results of the ABS approach on real-world data and discuss the framework.**

***Index Terms*—distributed radar fusion, multi-target tracking, background subtraction, radar ground stations**

I. Introduction

Maritime transport partakes in more than 80% of global trade today, putting focus on different sectors namely maritime safety and environment and infrastructure protection [1]. These emphasise the importance of maritime traffic monitoring and assessment, often facilitated by tracking systems built up on data fusion approaches based on sensors including radars, Automatic Identification System (AIS), lidars, and cameras amongst others [2]–[5]. Such frameworks encompass estimating a set of vessel state parameters recursively, known as target tracking, to provide traffic insights. Continuous data acquisition from radar ground stations nowadays increase reliability for traffic monitoring, offering wider coverage than lidars and cameras, given the radar's midrange resolution. Our framework is hence based on radar data streamed from distributed sensors which are then extracted as point clouds.

We establish two fundamental parts in our measurement (data) processing step, in order to distinguish between detection of potential vessels (including clutter) and that of infrastructure, referred to as background, when visible in the observation region (OR). The first part would, on one hand, contribute to METT which refers to the problem of estimating the extended states of multiple targets concurrently, given an unknown measurement-to-target association. This may lead to challenges of requiring restricted ORs, for instance, with gating strategies to exclude background measurements from the measurement set that is passed on to the tracker at a later stage [5]. On the other hand, the second part could provide sufficient prior knowledge about the background to not only improve vessel detection, but further extend the OR, eliminating the need of additional gating strategies or static masks. However, in busy port or inland waterways, it is common to find vessels moored over long periods at one berth before they are underway again, enough to be considered as background despite being temporarily stationary. Background detection methods should thus take into account such cases.

Tracking and mapping one's environment is central to Simultaneous Localization and Mapping (SLAM)-based applications [6]–[8], some of which are formulated as a dynamic object filtering (DOF) problem [9] with solutions implementing ray-tracing, visibility-based or segmentation-based approaches. Ray-tracing involves dividing the environment into voxel occupancy grids, where each voxel is updated based on laser ray hits and later classified according to a threshold. The approach by Hornung et al. [10] updates the occupancy probabilities of affected voxels upon receiving new sensor data. This probabilistic update considers the sensor's measurement accuracy and the likelihood that a voxel is occupied, free, or unknown. Similar probabilistic methods employ Bayesian occupancy grids or log-odds representations to update the background model as new point clouds are captured [11]. Despite the high accuracy of ray-tracing, it also requires significant computational resources.

Visibility-based methods are computationally less demanding and detect moving objects by monitoring changes in the distance to the nearest point observed by a sensor but are however, sensitive in occluded scenarios. Segmentation-based approaches, on the other hand, identify dynamic objects by categorising them according to predefined object types, thereby relying on pre-labelled ground truth (GT) data during training and are only able to recognise specific types of dynamic objects. While DOF identifies and eliminates moving measurements for precise mapping over time based on high resolution short range sensors (e.g. lidars), background detection and hence subtraction identifies and tracks moving targets based on mostly long range sensors (e.g. radar). As maritime traffic and port areas are prone to occlusions and lack GT, our motivation is towards implementing a probabilistic unsupervised ray-tracing method, with trade-offs for computation efficiency.

Our idea is to exploit information from previous observation steps by modelling local distributions of measurements in a spatially subdivided OR. Modelling background as a weak multinomial distribution (MD) estimation using random variables in non-stationary environments is presented in Stochastic

Learning-Based Weak Estimation (SLWE) [12]. It involves iteratively updating probabilistic estimates as new measurements emerge, hence potentially adapts to dynamic data distributions in the OR to reflect evolutions in the underlying distribution over time. By grouping radar measurements according to their spatial location and modeling them as a MD, the estimated probability of each pixel's measurement count evolves with incoming data. The frequency of observed measurement counts directly influences its corresponding probabilities: the higher the count at a given pixel, the higher its estimated probability becomes. The expected measurement count for each location can be inferred from the highest probabilities after some period. This enhances the probability of persistent measurements over time. If the measurement count with the highest probability within the MD for each location exceeds a given threshold, the pixel is classified as background. As such, the approach is entirely unsupervised, independent of GT, with an explainable model and suitable for our purpose.

By exploiting prior background knowledge adaptively, we improve vessel detection in conjunction to our ABS-METT framework and the overall traffic monitoring. To the best of the authors' knowledge, this is the first proposed application of weak MD-based background subtraction in a distributed radar tracking framework, by fusing data from ground stations and from an onboard sensor for METT. The contributions of this work are therefore two-fold,

- an adaptive approach, ABS, that uses MDs to model distributions of 2D radar points within pixels,
- an ABS-METT framework that fuses dynamic and static radar data,

for a reliable maritime traffic situation monitoring. Furthermore, as this work can be considered a continuation of that in [5], we therefore particularly emphasise on novelties that enhance the framework in this paper. We present the results and benefits with appropriate evaluation strategies.

The paper is structured as follows. In Section II, we define the framework problem at a high level, and explain our approaches in Section III. Results and the summary follow in Sections IV and V, respectively.

II. Problem Definition

At observation step k, a set $\boldsymbol{\mathcal{S}}_k$ of M number of 2D measurements each denoted by $\mathbf{z}$,

$$\boldsymbol{\mathcal{S}}_k = \left\{\mathbf{z}_k^j\right\}_{j=1}^{M} = \boldsymbol{\mathcal{S}}_k^G \cup \boldsymbol{\mathcal{S}}_k^O \tag{1}$$

is acquired from G ground stations around a certain OR. Sets $\boldsymbol{\mathcal{S}}_k^G = \bigcup_{g=1}^{G} \{\mathbf{S}\}_k^g$ and $\boldsymbol{\mathcal{S}}_k^O = \bigcup_{o=1}^{O} \{\mathbf{S}\}_k^o$ are the combined set of measurements from G ground stations and from O cooperating dynamic onboard radar sensors, respectively. Given $\boldsymbol{\mathcal{S}}_k$, we would like to obtain two subsets such that

$$\boldsymbol{\mathcal{B}}_k \subseteq \boldsymbol{\mathcal{S}}_k, \text{ and } \boldsymbol{\mathcal{Z}}_k \subseteq \boldsymbol{\mathcal{S}}_k, \tag{2}$$

where $\boldsymbol{\mathcal{B}}_k$ contains measurements that have been detected as potential background and $\boldsymbol{\mathcal{Z}}_k$ in turn results from a mask operation such that it contains the non-background measurements, assumed to be potential targets, including clutter. The following holds for the number of measurements after partitioning, $M = M^{\boldsymbol{\mathcal{B}}} + M^{\boldsymbol{\mathcal{Z}}}$, $M^{\boldsymbol{\mathcal{B}}}$ and $M^{\boldsymbol{\mathcal{Z}}}$ being the number of measurements in the respective subsets and $M^{\boldsymbol{\mathcal{B}}} >> M^{\boldsymbol{\mathcal{Z}}}$.

A. Exploiting Background Information

An MD is a generalisation of the binomial distribution to cater for more than two categories. Considering υ possible categories and assuming that each υ is mutually exclusive and each k independent, we define the MD as

$$\boldsymbol{\mathcal{Y}} \sim f(M_k, \boldsymbol{\psi}), \tag{3}$$

- $\boldsymbol{\psi} = (\psi_1, ..., \psi_\upsilon)$ represents the probabilities of observing each specific measurement count, where υ is maximum defined count, such that $\sum_{i=1}^{\upsilon} \psi_i = 1$,
- and $\boldsymbol{\mathcal{Y}} = (\mathcal{Y}_1, ..., \mathcal{Y}_\upsilon)$ has an MD function $f(.)$ so that $\sum_{i=1}^{\upsilon} \mathcal{Y}_i = M_k$.

The probability that $\boldsymbol{\mathcal{Y}} = (\mathcal{Y}_1, ..., \mathcal{Y}_\upsilon)$ takes some intensity value $y = (y_1, ..., y_\upsilon)$, has probability mass function given by

$$f_y = \frac{M_k!}{\prod_{i=1}^{\upsilon} y_i!} \prod_{i=1}^{\upsilon} \psi_i^{y_i}. \tag{4}$$

Given these probabilities, we identify areas that are most likely to have persistent measurement counts over time by examining the probabilities ψ_i with *i* = 1, ..., υ.

B. An METT Perspective

The state vector of a target t at k is given by

$$\boldsymbol{x}_k^t = \left[\mathbf{m}_k, \dot{\mathbf{m}}_k, \alpha_k, \ell_{1,k}, \ell_{2,k}\right]^T, \tag{5}$$

where $\mathbf{m}_k$ is the 2D position and $\dot{\mathbf{m}}_k$ the velocity; and extent state $\mathbf{p}_k$ comprises the orientation $\alpha_k \in [0, 2\pi)$, semi-axes lengths $\ell_{1,k}$ and $\ell_{2,k}$ (corresponding to t's length and width). T is the transpose operator. It was often found convenient to model radar-based targets as ellipses [4], [13], [14]. Elliptical measurement models, including the above, are usually integrated in trackers that are then broadly principled on data association-based or random finite set-based methods [3], [15] for METT.

The prior and posterior state densities, $p\left(\boldsymbol{x}_{k-1}^t | \boldsymbol{\mathcal{Z}}_{k-1}\right)$ and $p\left(\boldsymbol{x}_k^t | \boldsymbol{\mathcal{Z}}_k\right)$ respectively, are assumed to be Gaussians with zero-mean covariances. We would like to estimate the posterior multi-target state containing N_k targets, described as $\boldsymbol{\mathcal{X}}_k = \{\boldsymbol{x}_k^t\}_{t=1}^{N_k}$, given $\boldsymbol{\mathcal{Z}}_k$. From the formulation in [5],

$$p\left(\boldsymbol{\mathcal{X}}_k | \boldsymbol{\mathcal{Z}}_k\right) \propto \prod_{s=1}^{O+G} \prod_{t=1}^{N_k} p\left(\boldsymbol{\mathcal{Z}}_k^s | \boldsymbol{x}_k^t\right) p\left(\boldsymbol{x}_k^t | \boldsymbol{\mathcal{Z}}_{k-1}\right) \tag{6}$$

with the likelihood of target t given by $p\left(\boldsymbol{\mathcal{Z}}_k^s | \boldsymbol{x}_k^t\right)$ and predicted state density by $p\left(\boldsymbol{x}_k^t | \boldsymbol{\mathcal{Z}}_{k-1}\right)$, solutions based on the Kalman filter (KF) can be applied for recursively estimating the state.

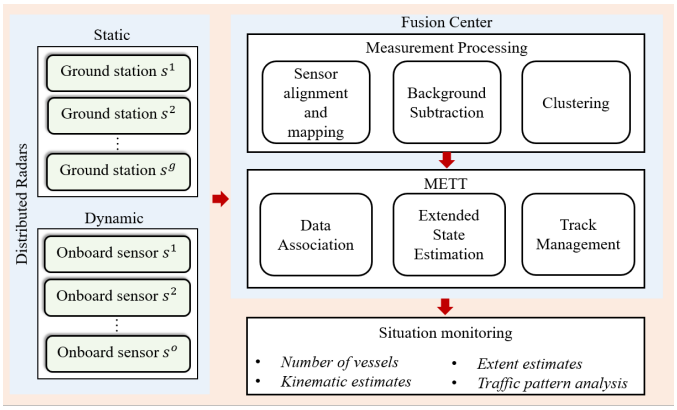

Fig. 1: Functional blocks in the framework.

III. The ABS-METT Framework

The proposed framework ABS-METT, which emphasises the integration of background subtraction for a distributed radar tracking system shown in Fig. 1, is an improvement over our previous work. The scope of this work lays in the custom implementation and added value of ABS in particular. Thorough details about the tracker's measurement and kinematic models are explained in the previous work [5]. A pseudocode of the core Fusion Centre is provided in Algorithm 1. The functional blocks are explained next. For brevity, sensor index s indistinguishably denotes static and dynamic sensors after the preprocessing step in III-A.

A. Sensor Alignment and Mapping

The implementation of our framework is based on the All-purpose structured EUROCONTROL surveillance information exchange (ASTERIX) protocol [16], allowing participating stations and vessels to exchange their own radar views through encoded messages. After being decoded, measurements from each sensor are converted and mapped onto a common reference frame in East North Up coordinates. Onboard measurements with a head-up setting are rotated and centred based on the most recent AIS true heading and position.

B. Background Subtraction

Multinomial-distributed random variables are used to represent probability distributions of υ radar measurement counts within pixels over time, where each pixel corresponds to a discretised OR. Rather than assuming a constant background per pixel, we model it as having multiple potential measurement counts over time, each associated with probability ψ. The likelihood of observing a particular measurement count i_{obs} at any step is governed by an MD.

At every consequent step, the background model in accordance to (3) for each pixel is updated to reflect its most probable measurement counts. The steps are explained as follows.

1) Model Initialisation: Each pixel in the OR is initialised at $k = 0$ with an MD probabilistic model such that

$$\psi_i(0) = \frac{1}{\upsilon}, \quad \forall i \in [1, \upsilon]. \tag{7}$$

Algorithm 1: Outline of ABS-METT at step k

Data:
- Set $\boldsymbol{\mathcal{S}}_k$ from s sensors, where $s = G + O$
- State prior $\widehat{\boldsymbol{x}}^t_{k-1}$, covariance $\mathbf{C}^{\boldsymbol{x},t}_{k-1}$ for each $t \in N_{k-1}$

Result: Estimate $\widehat{\boldsymbol{x}}^t_k$ and covariance $\mathbf{C}^{\boldsymbol{x},t}_k$

function update_bg_mask($\boldsymbol{\mathcal{S}}^s_k, \boldsymbol{\psi}$);
$\boldsymbol{\psi}_{1:\upsilon}(k+1)$ = update_prob($\boldsymbol{\mathcal{S}}^s_k$, α) acc. to (8)
$converged$ = euc_dist($\boldsymbol{\psi}(k+1), \boldsymbol{\psi}(k)$) acc. to (9)

Initialise hyperparameters (See Table III)
Initialise probs s.t. $\boldsymbol{\psi}_{1:\upsilon}(0) = \frac{1}{\upsilon}$

while *True* **do**
- $\boldsymbol{\mathcal{B}}^s_k \leftarrow$ update_bg_mask($\boldsymbol{\mathcal{S}}^s_k, \boldsymbol{\psi}(k)$)
- $\boldsymbol{\mathcal{B}}^s_k \leftarrow$ apply_threshold($\boldsymbol{\mathcal{B}}^s_k, \boldsymbol{\tau_M}$)
- **if** *converged* **then**
  - **for** *each* t **do**
    - KF state prediction $\left[\widehat{\boldsymbol{x}}^t_{k|k-1}, \mathbf{C}^{\boldsymbol{x},t}_{k|k-1}\right]$ = predict$\left(\widehat{\boldsymbol{x}}^t_{k-1}, \mathbf{C}^{\boldsymbol{x},t}_{k-1}\right)$
  - **end**
  - **for** *each* s **do**
    - Extract measurements using latest mask
    - $\boldsymbol{\mathcal{Z}}^s_k \leftarrow \mathbf{S}^s_k \cap \overline{\boldsymbol{\mathcal{B}}}_k$
    - Cluster measurements
    - $\widetilde{\boldsymbol{\mathcal{Z}}}^s_k, c_k \leftarrow$ dbscan($\boldsymbol{\mathcal{Z}}^s_k, \epsilon, min\_points$)
    - **if** t *is confirmed* **then**
      - Association probabilities $\left[\{\beta_{jt}\}^{c_k}_{j=0}\right]$ = get_prob$\left(\{\tilde{\mathbf{z}}_j\}^{c_k}_{j=1}, \mathbf{C}^{\tilde{\mathbf{z}}}, \lambda, P_D\right)$
      - KF state update $\left[\widehat{\boldsymbol{x}}^t_{k|k}, \mathbf{C}^{\boldsymbol{x},t}_{k|k}\right]$ = update$\left(\widehat{\boldsymbol{x}}^t_{k|k-1}, \mathbf{C}^{\boldsymbol{x},t}_{k|k-1}, \widetilde{\boldsymbol{\mathcal{Z}}}^s_k\right)$
    - **end**
  - **end**
  - Output:
    - Posterior state $\widehat{\boldsymbol{x}}^t_{k|k}$, covariance $\mathbf{C}^{\boldsymbol{x},t}_{k|k}$
    - $\boldsymbol{\mathcal{Z}}_k$ for evaluation
- **end**

end

2) Update Process (Stochastic Learning): As new frames are received, the model probabilistically updates the probability of occurrence of each measurement count i. Using the following update rule [12] and observed count i_{obs},

$$\psi_i(k+1) = \begin{cases} \alpha \cdot \psi_i(k) + (1-\alpha), & \text{if } i = i_{obs} \\ \alpha \cdot \psi_i(k), & \text{otherwise.} \end{cases} \tag{8}$$

where $\psi_i(k)$ is the probability of getting measurement count i, $\alpha \in [0, 1]$ is the learning rate which controls how quickly the model adapts to recent observations. ψ_i is increased if it is observed at $k+1$, while probabilities for other counts are scaled down by α.

3) Estimation of Foreground/Background: For each pixel, the model obtains an MD over its possible measurement counts. We classify a pixel as background if the most likely measurement count in the updated distribution exceeds a given threshold. Otherwise, it is classified as foreground, that is, targets and clutter. These classifications result in sets $\boldsymbol{\mathcal{B}}$ (background) and $\boldsymbol{\mathcal{Z}}$ (foreground) respectively.

4) Convergence: We denote the first moment of the Euclidean distance between two MDs vectors $\boldsymbol{\psi} = [\psi_1, \ldots, \psi_v]$ and $\boldsymbol{\psi}' = [\psi'_1, \ldots, \psi'_v]$ by

$$d(\boldsymbol{\psi}, \boldsymbol{\psi}') = \sqrt{\sum_{i=1}^{v} (\psi_i - \psi'_i)^2}, \tag{9}$$

where ψ_i and ψ'_i are the probabilities of the i-th measurement count in the respective MDs. As (9) is theoretically guaranteed to converge over time [12], we can ascertain that the underlying distribution has been learned after a specific duration. This criterion is used to initiate the tracker (see II).

C. Clustering and Data Association

Using DBSCAN [17] on $\boldsymbol{\mathcal{Z}}$, we obtain set $\widetilde{\boldsymbol{\mathcal{Z}}} = \{\tilde{\mathbf{z}}_j\}_{j=1}^{c}$ of c arbitrarily shaped clusters with centroids $\tilde{\mathbf{z}}_j$ as input to the tracker. Each cluster corresponds to point clouds originating either from a particular vessel or clutter, that may include False Negative (FN) from ABS (See IV-C). With the Joint Probabilistic Data Association (JPDA) scheme [15], every cluster j-to-target t's marginal association probabilities β_{jt} are calculated based on density $\mathbf{C}^{\tilde{\mathbf{z}}_j}$, the probability of detection P_D and clutter density λ. These are finally used to approximate target t's posterior density.

D. METT

Our tracker is essentially a JPDA filter with an extended state and elliptical measurement models. Based on recursive Bayesian estimation, the three major steps at k are:

- predicting target state at $k+1$,
- calculating marginal association probabilities $\boldsymbol{\beta}$, and,
- updating state weighted according to the probabilities.

A module for track management runs in parallel to cater for track initialisation and pruning.

IV. Results and Analyses

In this section, we explain the scenarios of interest implemented via simulation and evaluate our proposed framework. We also include some findings from real-world data.

A. Experimental Set Up

We designed and ran our scenarios on inVNE [18]. The simulation area was located in the Port of Hamburg. It involved 3 ground stations and 1 radar sensor aboard a law enforcement vessel *V1* which proceeded downstream in close proximity to other vessels. All 4 sensors were collaboratively broadcasting their observations over ASTERIX links. There were 3 additional non-collaborative vessels in the area. Table I contains relevant vessel particulars of the simulated fleet.

TABLE I: Vessel Name, Dimension, and Trajectory

Vessel	L × W [m]	Trajectory Specifics
DLR4 (V1)	25.5 x 6	Dynamic throughout
ACS Diamond (V2)	190 x 32	Moored for first half before heading on course
Evelyn Maersk (V3)	397 x 56.4	Dynamic from beginning and moors at the end
Thames Highway (V4)	148 x 25	Dynamic throughout

TABLE II: Framework Approaches

Case		Sensors	Description
1	A	Static	Tracking starts upon convergence
	B	Static and Dynamic	
2	A	Static	Tracking from beginning
	B	Static and Dynamic	

The distributed system as observed by all collaborating parties had 2 vessels at first, *V3* and *T. Highway*, both underway on reciprocal courses. Inbound, *V3* proceeded upstream to her berth and passed *V2* which was moored port alongside and scheduled for departure. *V2* unberthed once *V3* was past and clear. There were situations of occlusion causing part of the fleet to be overshadowed by one another. *V1* remained within the OR to provide an "inner" view from a central part that is prone to occlusions for ground stations. We executed our framework in 4 settings (Table II) to investigate conditions and assess the framework's performance, with parameters from Table III.

Plots from the framework are illustrated in Fig. 2. The first column is the output of ABS, with black points as background and red ones as targets. GT-based bounding boxes corresponding to vessels are also plotted. The other columns are tracker output for both cases. At $k = 900$s, *V2* is classified as background. The tracker detects the remaining vessels except for *V1* which did not pass the min_points for clustering due to occlusions. At $k = 999$s as *V2* starts to unberth, all vessels are correctly tracked. When *V3* starts mooring at $k = 2085$s, a gradual transition to background is seen as the extent shrinks over time. However, errors are introduced in Case B because *V1* yields noisy measurements, challenging the background's convergence. Since the moving threshold τ_M filters out weak and noisy detections, this problem can be addressed by increasing τ_M at the cost of misdetecting smaller vessels. Hence, we chose these hyperparameter values as a trade-off based on experimental evaluation.

B. Evaluation and Discussion

We define a confusion matrix in Table IV. Using AIS-based vessel position, dimension and heading, bounding boxes are generated as GT. Measurements falling inside them (blue ones in Fig. 2) relate to actual targets, i.e. FP and TN, while those outside to actual background, i.e. TP and FN.

At each k, sets $\boldsymbol{\mathcal{B}}_k$ and $\boldsymbol{\mathcal{Z}}_k$ obtained from ABS algorithm are compared to the bounding boxes. The metrics considered, *False Positive Rate* and *Negative Predicted Value*, are defined

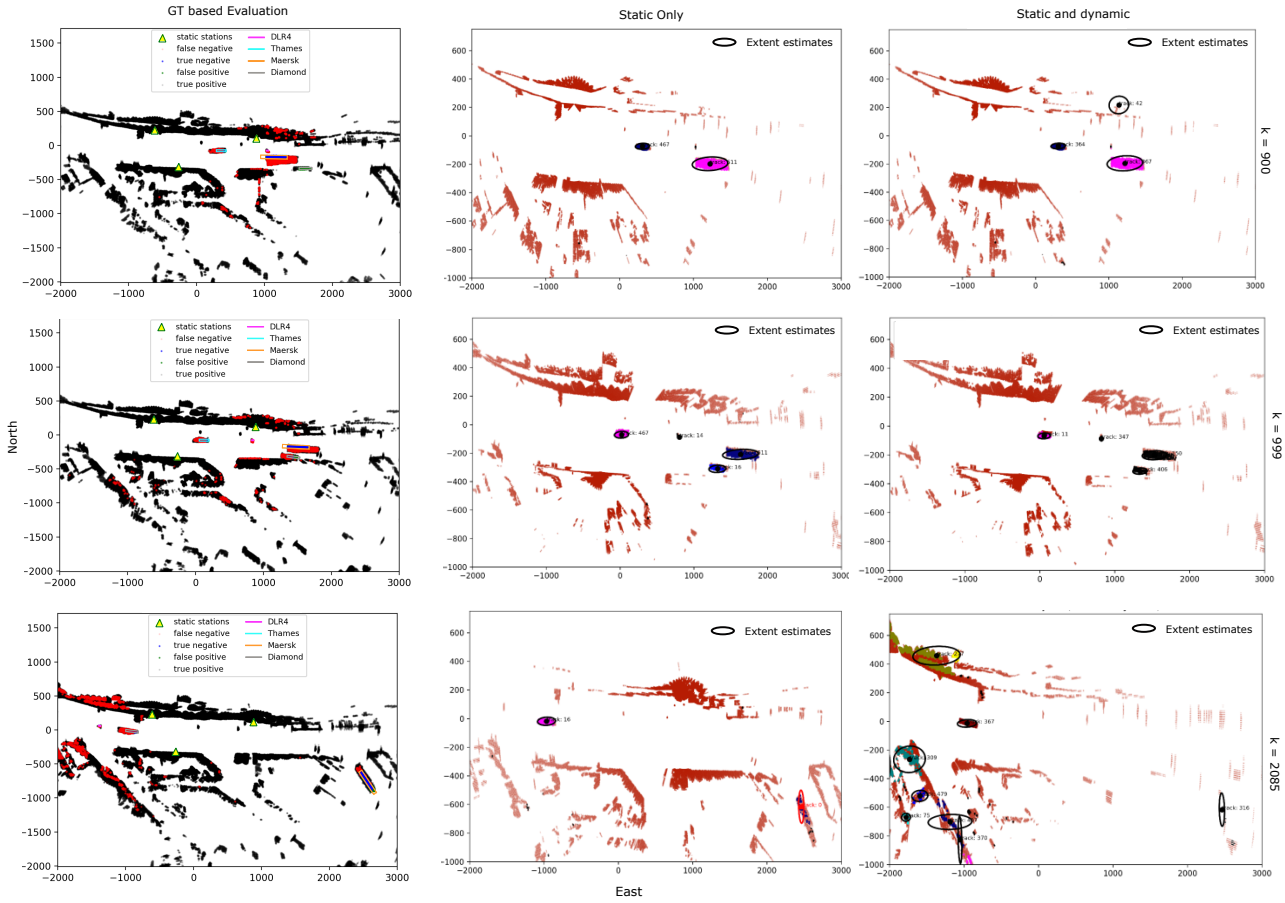

Fig. 2: First column shows output of ABS evaluated against GT and the positions of the distributed ground stations. The remaining columns are the tracker's output in both cases. The rows correspond to $k = 900, 999$, and 2085 respectively.

TABLE III: Hyperparameter values

Step	**Background Subtraction**				**DBSCAN**		**JPDA Filter**	
Parameter	Learning rate α	#pixels	Measurement count υ	Moving threshold τ_M	min_points	ϵ	Clutter density λ	Detection prob. P_D
Value	0.9	1000^2	256	5	130	65	3	0.85

TABLE IV: Confusion Matrix at k

Class	Est. Background	Est. Potential Targets
Background	True Positive (TP)	FN
Potential Targets	False Positive (FP)	True Negative (TN)

as, $FPR = \dfrac{FP}{FP+TN}$ and $NPV = \dfrac{TN}{TN+FN}$. Low *FPR* values means a low probability of misdetection, while high *NPV* values signify better METT performance.

Fig. 3 shows the above metrics calculated for cases 2 over time. Cases 1 are excluded as they only differ in the tracker's initiation. The first 250s shows the adaptive nature of ABS as measurements initially classified as FP change to TN when targets move, rapidly improving both metrics. After 500s, *V3* has nearly radial heading against at least 2 sensors so her measurements persist long enough to be classified as background, thus raising *FPR*. The figure also shows further

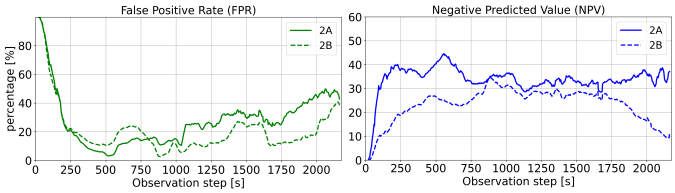

Fig. 3: *FPR* and *NPV* for cases 2A (solid) and 2B (dashed).

increase in *FPR* after 1750s when *V3* moors and gets gradually classified as background. *V1*'s measurements improve overall target visibility in B-scenarios, hence the lower *FPR* metric. *V3* points, however, do not last enough to be classified as such, thereby increasing the number of FNs and reducing *NPV* especially as it heads towards an area with reduced fused coverage, shown in the lower left plot in Fig. 2. The results

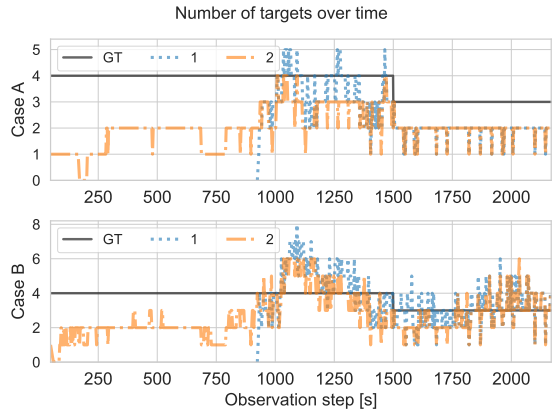

Fig. 4: Estimated number of target against GT

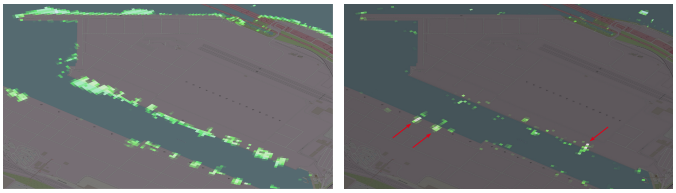

(a) Background mask (b) False negatives on land

Fig. 5: ABS on real-world data.

emphasise the challenges of hyperparameter tuning to resolve trade-offs between low *FPR* and high *NPV*.

The impact of ABS on the tracker's performance can be seen in Fig. 4 where the tracker experiences more misdetections when it starts before ABS converges in 2A and 2B. After convergence, all cases show fewer misdetections, especially when *V1* is present. The fluctuations are due to false tracks lasting a few seconds before deletion.

C. Application on Real World and Challenges

The ABS approach was applied in real-world ASTERIX data recorded for 1.5 hours in Hamburg port (Fig. 5), covering a docking area as well intense traffic of different vessel types. The lack of labels in the dataset does not allow assessing the algorithm performance, however a qualitative analysis was carried out and additional challenges were identified. In particular the presence of dynamic points caused by the movement of gantry cranes traversing the length of a quay and the shadows on background created by large vessels passing close to the radar station, both raising the number of FN, making more difficult tuning the hyper-parameters to eliminate such points while still correctly detecting smaller vessels.

V. Summary

In this work we presented an METT framework which integrates an adaptive background subtraction approach in distributed radar systems. The proposed framework was implemented and evaluated over simulated data from static and dynamic sensors. The results show two major benefits. Firstly, exploiting dynamic sensors yields increased visibility in occlusion prone regions covered solely by ground stations. Secondly, we have an improved target detection over a widened OR without manual gating strategies. We also ran our approach on real-world data and highlighted the delicacy of parameter tuning, given the interdependency of framework components. Our next work will therefore focus on hyperparameter optimisation for real-world applications.

References

[1] European Maritime Safety Agency (EMSA), "EMSA Facts and Figures," 2023. EMSA Highlights 2023.

[2] Øystein Kaarstad Helgesen, K. Vasstein, E. F. Brekke, and A. Stahl, "Heterogeneous Multi-Sensor Tracking for an Autonomous Surface Vehicle in a Littoral Environment," *Ocean Engineering*, vol. 252, 2022.

[3] J. Koch, "Bayesian Approach to Extended Object and Cluster Tracking using Random Matrices," *IEEE Transactions on Aerospace and Electronic Systems*, vol. 44, no. 3, pp. 1042–1059, 2008.

[4] G. Vivone and P. Braca, "Joint Probabilistic Data Association Tracker for Extended Target Tracking Applied to X-Band Marine Radar Data," *IEEE Journal of Oceanic Engineering*, pp. 1007–1019, January 2015.

[5] J. S. Fowdur, M. Baum, F. Heymann, and P. Banyś, "An Overview of the PAKF-JPDA Approach for Elliptical Multiple Extended Target Tracking Using High-Resolution Marine Radar Data," *Remote Sensing*, vol. 15, no. 10, 2023.

[6] A. Macario Barros, M. Michel, Y. Moline, G. Corre, and F. Carrel, "A Comprehensive Survey of Visual SLAM Algorithms," *Robotics*, vol. 11, no. 1, 2022.

[7] I. Abaspur Kazerouni, L. Fitzgerald, G. Dooly, and D. Toal, "A Survey of State-of-the-Art on Visual SLAM," *Expert Systems with Applications*, vol. 205, 2022.

[8] L. Hösch, A. Llorente, X. An, J. P. Llerena, and D. Medina, "High Definition Mapping for Inland Waterways: Techniques, Challenges and Prospects," in *IEEE 26th International Conference on Intelligent Transportation Systems (ITSC)*, pp. 6034–6041, IEEE, 2023.

[9] H. Peng, Z. Zhao, and L. Wang, "A Review of Dynamic Object Filtering in SLAM Based on 3D LiDAR," *Sensors*, vol. 24, no. 2, 2024.

[10] A. Hornung, K. M. Wurm, M. Bennewitz, C. Stachniss, and W. Burgard, "OctoMap: An Efficient Probabilistic 3D Mapping Framework based on Octrees," *Springer Autonomous Robots*, vol. 34, pp. 189–206, 2013.

[11] J. Gehrung, M. Hebel, M. Arens, and U. Stilla, "An Approach to Extract Moving Objects from MLS Data using a Volumetric Background Representation," *ISPRS Annals of the Photogrammetry, Remote Sensing and Spatial Information Sciences*, vol. IV-1/W1, pp. 107–114, 2017.

[12] L. R. B. John Oommen, "Stochastic Learning-based Weak Estimation of Multinomial Random Variables and its Applications to Pattern Recognition in Non-Stationary Environments," *Pattern Recognition*, vol. 39, no. 3, pp. 328–341, 2006.

[13] S. K. Joshi, S. V. Baumgartner, and G. Krieger, "Tracking and Track Management of Extended Targets in Range-Doppler Using Range-Compressed Airborne Radar Data," *IEEE Transactions on Geoscience and Remote Sensing*, vol. 60, pp. 1–20, 2022.

[14] J. S. Fowdur, M. Baum, and F. Heymann, "Tracking Targets with Known Spatial Extent Using Experimental Marine Radar Data," in *IEEE 22nd International Conference on Information Fusion (FUSION)*, pp. 1–8, 2019.

[15] B.-N. Vo, M. Mallick, Y. Bar-Shalom, S. Coraluppi, R. Osborne III, R. Mahler, and B.-T. Vo, "Multitarget Tracking," *Wiley Encyclopedia*, pp. 1–25, 09 2015.

[16] EUROCONTROL, "EUROCONTROL Specification for Surveillance Data Exchange - Part 1 All Purpose Structured EUROCONTROL Surveillance Information Exchange (ASTERIX)." Online: https://www.eurocontrol.int/asterix.

[17] M. Ester, H.-P. Kriegel, J. Sander, and X. Xu, "A Density-based Algorithm for Discovering Clusters in Large Spatial Databases with Noise," in *Proceedings of the Second International Conference on Knowledge Discovery and Data Mining*, KDD'96, p. 226–231, AAAI Press, 1996.

[18] in-innovative navigation GmbH, "Vessel Traffic Simulator and Sensor Data Generator." URL: https://www.innovative-navigation.de/en/products/simulation/, [Accessed: 11-15-2024].